


## Model of Magnetic Damping and Anisotropy at Elevated Temperatures: Application to Granular FePt Films

Mara Strungaru<sup>✉</sup>,\* Sergiu Ruta, Richard F.L. Evans<sup>✉</sup>, and Roy W. Chantrell<sup>✉</sup>  
*Department of Physics, University of York, York YO10 5DD, United Kingdom*

 (Received 10 February 2020; revised 26 March 2020; accepted 26 May 2020; published 24 July 2020)

An understanding of the damping mechanism in finite-size systems and its dependence on temperature is a critical step in the development of magnetic nanotechnologies. In this work, nanosized materials are modeled via atomistic spin dynamics, the damping parameter being extracted from ferromagnetic resonance (FMR) simulations applied for FePt systems, generally used for heat-assisted magnetic recording media (HAMR). We find that the damping increases rapidly close to  $T_C$  and the effect is enhanced with decreasing system size, which is ascribed to scattering at the grain boundaries. Additionally, FMR methods provide the temperature dependence of both damping and the anisotropy, which are important for the development of HAMR. Semianalytical calculations show that, in the presence of a grain-size distribution, the FMR line width can decrease close to the Curie temperature due to a loss of inhomogeneous line broadening. Although FePt has been used in this study, the results presented in the current work are general and valid for any ferromagnetic material.

DOI: [10.1103/PhysRevApplied.14.014077](https://doi.org/10.1103/PhysRevApplied.14.014077)

### I. INTRODUCTION

The magnetic damping parameter is important from both a fundamental and applications point of view, as it controls the dynamic properties of the system, such as magnetic relaxation, spin waves, domain-wall propagation, and magnetic reversal processes. Magnetic materials have a broad range of interest for nanodevices and/or nanoelements and exhibit a fast response to external excitations. In information technologies, damping plays a crucial role, especially for spin-transfer torque magnetic random-access memories (STT-MRAM), where it controls the switching current [1]. With the emerging field of magnetization switching via ultrafast laser pulses, the damping parameter can affect the fluence of the laser pulse necessary for demagnetizing and switching of the sample [2]. Spintronic devices such as racetrack memories, which are based on domain-wall propagation in magnetic nanowires, are also influenced by damping [3]. As present-day magnetic technologies are based on nanostructures of smaller and smaller sizes, the finite-size effects become more important and can significantly influence the magnetic properties, including the damping. Therefore, an understanding of the dependence of damping on temperature in finite-size systems is a critical step in the development of magnetic nanotechnologies.

One of the technologies that is strongly influenced by damping is magnetic recording, where the damping

constant of the storage medium controls the writing speeds and bit error rates [4,5]. The next generation of ultrahigh-density storage technology is likely to be based on heat-assisted magnetic recording (HAMR) [6–9]. The main candidate for HAMR media is  $L1_0$ -ordered FePt [8,10], due to its large perpendicular anisotropy and low Curie temperature ( $T_C$ ). For HAMR applications, information is stored at room temperature (300 K) but the writing is done at elevated temperatures close to  $T_C$ , therefore providing a large range over which the temperature dependence of the damping needs to be understood. As the areal density increases, the grain size decreases and finite-size effects become crucial. For this reason, FePt is an ideal candidate for studying temperature and finite-size effects on the damping. Although FePt has been used in this study, the results presented in the current work are general and valid for any ferromagnetic material.

The first investigations of the Gilbert damping for FePt have involved experimental measurements via optical pump-probe techniques. The damping measured at room temperature varies widely from one study to another. Becker *et al.* [11] have reported an effective damping of 0.1 and an even larger value (0.21) has been found by Lee *et al.* [12], while the measurements of Mizukami *et al.* [13] have given a value of 0.055. It is important to note that these values include both intrinsic and extrinsic contributions, the purely intrinsic damping being even smaller than the reported values [13,14]. Recently, Richardson *et al.* [15] have reported experimental measurements of damping at elevated temperatures showing an unexpected decrease

\*mss555@york.ac.uk

of damping with temperature. A decrease in the effective damping can be crucial in HAMR, as this can increase the switching time, affect the signal-to-noise ratio, and negatively impact the performance of HAMR. The damping variation at elevated temperatures and in finite-sized systems is therefore a critically important problem to be addressed especially by means of theoretical studies.

Ostler *et al.* [16] have successfully calculated the temperature dependence of damping in FePt bulk and thin-film systems based on the Landau-Lifshitz-Bloch (LLB) equation [17], showing an increased damping for thin-film systems in comparison with the bulk case. The LLB equation is derived for a bulk material. It is important to note that a major contribution to damping, especially at elevated temperatures, arises from magnon scattering. On the bulk scale, these processes are reproduced by the LLB equation, but with decreasing linear dimension, finite-size and surface effects become important. Since these are not accounted for by the LLB equation, it is necessary to use atomistic-spin-dynamics (ASD) simulations [18] for nanoscale grains, as ASD calculations include magnon processes. Using ASD, we are able to calculate the ferromagnetic resonance (FMR) spectra for small system sizes at elevated temperatures. Ferromagnetic resonance simulations are computationally very expensive; hence we develop a more efficient method of calculating the damping of these systems via a grid-search method. We show that both of the methods agree and, furthermore, that they are able to calculate both the dependence of damping and anisotropy as functions of the temperature. The dependence of anisotropy as a function of the temperature is crucial for HAMR, as it defines the temperature at which the writing process occurs.

## II. FERROMAGNETIC RESONANCE USING ATOMISTIC SPIN DYNAMICS

To calculate damping as a function of the temperature, we perform ASD simulations using the software package VAMPIRE [18]. ASD simulations assume a fixed lattice of atoms with which is associated a magnetic moment or spin  $\mathbf{S}_i = \boldsymbol{\mu}_i/\mu_s$  that can precess in an effective field  $\mathbf{H}_i$  according to the Landau-Lifshitz-Gilbert (LLG) equation. In our model, the Hamiltonian of the system contains a Heisenberg exchange term of strength  $J_{ij}$ , uniaxial energy of strength  $k_u$ , and a Zeeman term as follows:

$$\mathcal{H} = -\frac{1}{2} \sum_{i,j} J_{ij} (\mathbf{S}_i \cdot \mathbf{S}_j) - k_u \sum_i (\mathbf{S}_i \cdot \mathbf{e})^2 - \sum_i \mu_i (\mathbf{S}_i \cdot \mathbf{B}). \quad (1)$$

The effective field can be calculated from the Hamiltonian of the model, to which we add a thermal noise  $\xi_i$ , which

acts as a Langevin thermostat:

$$\mathbf{H}_i = -\frac{1}{\mu_i \mu_0} \frac{\partial \mathcal{H}}{\partial \mathbf{S}_i} + \xi_i. \quad (2)$$

The thermal field is assumed to be a white noise, with the following mean, variance, and strength, as calculated from the Fokker-Planck equation:

$$\langle \xi_{i\alpha}(t) \rangle = 0, \quad \langle \xi_{i\alpha}(t) \xi_{j\beta}(s) \rangle = 2D \delta_{\alpha,\beta} \delta_{ij} \delta(t-s), \quad (3)$$

$$D = \frac{\lambda k_B T}{\gamma \mu_i \mu_0}, \quad (4)$$

where  $\lambda$  represents the coupling to the heat bath,  $T$  is the thermostat temperature, and  $\gamma$  is the gyromagnetic ratio. We note that the heat-bath coupling constant  $\lambda$  is different from the effective Gilbert damping  $\alpha$ , as the latter includes contributions from magnon scattering and other extrinsic processes such as inhomogeneous line broadening.

After calculating the effective field that acts on each atom, the magnetization dynamics are given by solving the LLG equation [Eq. (5)] applied at the atomistic level [19], using a numerical integration based on the Heun scheme:

$$\frac{\partial \mathbf{S}_i}{\partial t} = -\frac{\gamma}{(1+\lambda^2)} \mathbf{S}_i \times (\mathbf{H}_i + \lambda \mathbf{S}_i \times \mathbf{H}_i). \quad (5)$$

To calculate the damping using ASD, we apply an out-of-plane magnetic field ( $B$ ) to the sample with an additional in-plane oscillating field [ $B_{rf} = B_0 \sin(2\pi \nu t)$ ], which is the default setup for ferromagnetic resonance experiments. The oscillating field will induce a coherent precession of the spins of the system, which will result in an oscillatory behavior of the in-plane magnetization. By sweeping the frequency of the in-plane field, the amplitude of the oscillations of magnetization will change, with a maximum corresponding to the resonance frequency (as shown in Fig. 1). By Fourier transformation of the in-plane magnetization, the power spectrum as a function of the frequency is obtained. Figure 1 shows the FMR spectra for a single spin of FePt at 0 K. The spectra can be fitted by a Lorentzian curve [Eq. (6)], where  $w$  represents the width of the curve and  $A$  its amplitude. By fitting with Eq. (6), the effective Gilbert damping  $\alpha$  and resonance frequency  $f_0$  can be extracted:

$$L(x) = \frac{A}{\pi} \frac{0.5w}{(x-f_0)^2 + (0.5w)^2}, \quad \alpha = \frac{0.5w}{f_0}. \quad (6)$$

The model parameters for FePt are listed in Table I.  $L1_0$  FePt has a face-centered tetragonal structure formed of alternating layers of Fe and Pt, which can be approximated to a body-centered tetragonal structure with the

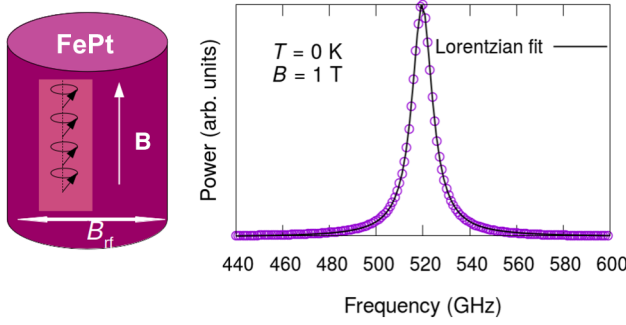


FIG. 1. An illustration of the setup used for ferromagnetic resonance experiments. An out-of-plane magnetic field ( $B$ ) and an in-plane oscillating field [ $B_{rf} = B_0 \sin(2\pi \nu t)$ ] are applied to the sample, as shown in the right inset. The power spectrum is obtained, as a function of the frequency, by Fourier transformation of the in-plane magnetization. The simulation is performed for a single FePt spin at  $T = 0\text{K}$ , having a damping of 0.01. This is equivalent to simulating a macrospin at  $T = 0\text{K}$  with equivalent properties. By fitting the power spectrum, the input resonance frequency and damping can be reproduced.

central site occupied by Pt. The *ab initio* calculations by Mryasov *et al.* [20] have shown that the Pt spin moment is found to be linearly dependent on the exchange field from the neighboring Fe moments. This dependence allows the Hamiltonian to be written only considering the Fe degrees of freedom. Under these assumptions, by neglecting the explicit Pt atoms, the system can be modeled as a simple cubic tetragonal structure, with each atomic site corresponding to an effective Fe+Pt moment. To minimize the computational cost of the FMR calculations, the model used for the FePt system is restricted only to nearest-neighbor interactions, in contrast with the full Hamiltonian given by Mryasov *et al.* [20]. The nearest-neighbor exchange value is chosen to give a Curie temperature of FePt of 720 K, to be in agreement with reported values for the nearest and the long-range exchange magnetic Hamiltonian [21]. The damping parameter has been chosen to approximate the experimentally measured value in recording media provided by the Advanced Storage Research Consortium (ASRC). The  $L1_0$  phase of FePt has a very large uniaxial anisotropy; hence the increased thermal stability of the grains. The uniaxial anisotropy used in

TABLE I. The parameters used for the initial calculations of the damping constant of FePt.

Quantity	Symbol	Value	Units
Nearest-neighbor exchange	$J_{ij}$	$6.71 \times 10^{-21}$	J
Anisotropy energy	$k_u$	$2.63 \times 10^{-22}$	J
Magnetic moment	$\mu_S$	3.23	$\mu_B$
Thermal-bath coupling	$\lambda$	0.05	
DC perpendicular field	$B$	1	T
RF in-plane field	$B_{rf}$	0.05	T

the simulation gives a anisotropy field of  $H_k = 2k_u/\mu_s = 17.55\text{ T}$ , slightly larger than the value used by Ostler *et al.* (15.69 T). The FMR fields (0.05 T) used in our simulations are generally larger than experimental FMR fields to allow more accurate simulations with enhanced temperature. Our tests confirm that no nonlinear modes are excited during the FMR simulations.

At  $T = 0\text{ K}$ , the damping we extract from the FMR spectrum should correspond to the input coupling  $\lambda$ , as no thermal scattering effects are present; hence the effective damping of the system is given by the Gilbert damping, which is the coupling to the heat bath. For this simulation, we use an input heat-bath constant of  $\lambda = 0.01$ , which we then recover by performing FMR calculations at  $T = 0\text{ K}$ , a method that serves as verification of our model. The damping obtained agrees to within a 0.1% fitting error. The resonance peak should appear exactly at the resonance frequency given by the Kittel formula,  $f_{\text{Kittel}} = \gamma/2\pi(B + 2k_u/\mu_s)$ , depending on the applied field strength ( $B$ ) and on the perpendicular anisotropy of our system, ( $H_k = 2k_u/\mu_s$ ). For an FePt system, the resonance frequency we obtain is 520 GHz to within a 1% fitting error, due to the exceptionally large magnetic anisotropy of the system.

### III. GRID-SEARCH METHOD

The Gilbert damping can be also calculated by fitting the time traces of the magnetization relaxation. The time traces can be obtained via pump-probe experiments [11]; however, the dynamics of the magnetization will include the effect of the laser pulse, such as heating and induced local magnetization due to the inverse Faraday effect. To avoid the contributions to the damping from the laser pulse, the damping can be calculated by taking the system out of equilibrium, letting it relax, and subsequently recording the time trace of the magnetization. Ellis *et al.* [22] have numerically studied the damping of rare-earth-doped permalloy using transverse relaxation curves, by fitting them with the analytical solutions of the LLG equations. In the case of large anisotropy, exchange interaction, and an applied field, there is no simple general solution to the LLG equation. Pai *et al.* [23] have used an applied field that is much larger than the anisotropy field, so that the dynamics closely approximate those of the LLG equation with no anisotropy. However, this approach is unsuitable for FePt, due to the very large fields required and also the influence of strong magnetic fields near the Curie temperature. Hence, we adopt a computational grid-search method, where we precalculate single-spin solutions for the LLG equation using ASD, build a database using these solutions, and then build an algorithm that can identify the damping and anisotropy parameters from any transverse relaxation curve. The method we choose simply involves sweeping through the parameter space, the solution being

given by minimizing the sum of the squared residuals, a method known as grid search.

The grid-search method can be used to fit time-dependent  $m(t)$  curves in the case where analytical solutions do not exist. The numerical curves that need to be fitted are compared with each of the precalculated numerical curves with the single-spin system. The best match will be given by the curve with the lowest sum of squared residuals, the  $\chi^2$  parameter, where  $\chi^2$  is defined as

$$\chi^2 = \sum_{i=1}^N \left[ m_i(t^i) - f(t^i, \mathbf{p}) \right]^2, \quad (7)$$

in which  $m_i(t^i)$  is the value of the magnetization at each moment in time  $t^i$ ,  $f(t^i, \mathbf{p})$  are the precalculated single-spin dependencies of the magnetization at each moment  $t^i$ , and  $\mathbf{p}$  is the list of parameters that have been varied [in our case,  $\mathbf{p} = (k_u, \alpha)$ ]. The minimum value of  $\chi^2$  from all  $\mathbf{p}$  parameters is the best-agreement numerical solution.

Figure 2 shows the calculated  $\chi^2$  as a function of the main parameters, specifically the anisotropy and damping, at  $T = 0.1$  K. In order to construct the single-spin simulation database, we choose a resolution of  $\Delta k_u = 0.015 \times 10^{-22}$  J for the anisotropy and  $\Delta \alpha_{\text{step}} = 0.001$  for the damping. It can be seen that the anisotropy is very well resolved: there is a sharp minimum at  $k_u = 2.625 \times 10^{-22}$ , which is the closest value to the input anisotropy,  $k_u = 2.63 \times 10^{-22}$  taking into account the resolution that we use for the database. In the case of damping, the minimum is wider, leading to an error of approximately 0.017 in determination of the damping, which is slightly larger than the resolution used in the construction of the database.

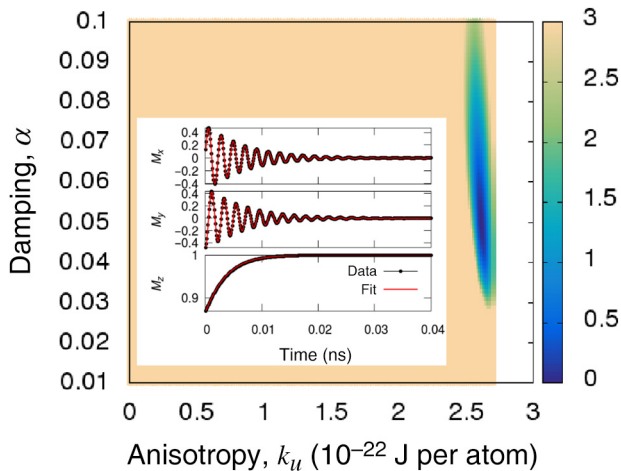


FIG. 2. The  $\chi^2$  map calculated using the grid-search method based on single-spin simulations at  $T = 0.1$  K. The inset depicts the input and fitted magnetization relaxation curves showing the validation of the method.

#### IV. HIGH-TEMPERATURE FMR: DAMPING AND ANISOTROPY CALCULATIONS

In this section, the damping and anisotropy are computed from frequency-dependent FMR spectra and via the grid-search method. The aim is to investigate the damping close to  $T_c$  and, in particular, the effect of finite grain size. First, we test the effectiveness of the grid-search method that is presented in Sec. III. Figure 3 shows the comparison between the two methods of calculation of the damping as a function of the temperature for a granular system of 15 noninteracting grains of diameter 5 nm and height 10 nm. The variations of anisotropy with temperature agree very well between the two methods; however, the grid-search method is far more computationally efficient. The enhanced computational efficiency comes from the fact that instead of simulating multiple frequency points to obtain the FMR, a single transverse relaxation simulation is needed to calculate the same parameters. The time scales for the two simulations are also different: the frequency-dependent FMR requires around 3 ns for each data point in the FMR spectra to perform the FFT analysis, while the transverse relaxation method requires, depending on the material, less than 1 ns. The extracted damping values agree reasonably well between the two methods, within the error bars. For the grid-search method, there will be a damping interval that gives the same value of  $\chi^2$ . For the FMR experiment, the error bar is computed as the standard error of groups of five noninteracting grains.

Because of the large error bars, especially close to  $T_c$  for the grid-search method, we use the direct FMR simulations for the remainder of the paper and later consider possible means of improvement of the reliability of the grid-search method. For our initial calculations, we model a granular FePt system as a cylinder of height 10 nm and diameter 5 nm. For comparison, the bulk FePt system is modeled via

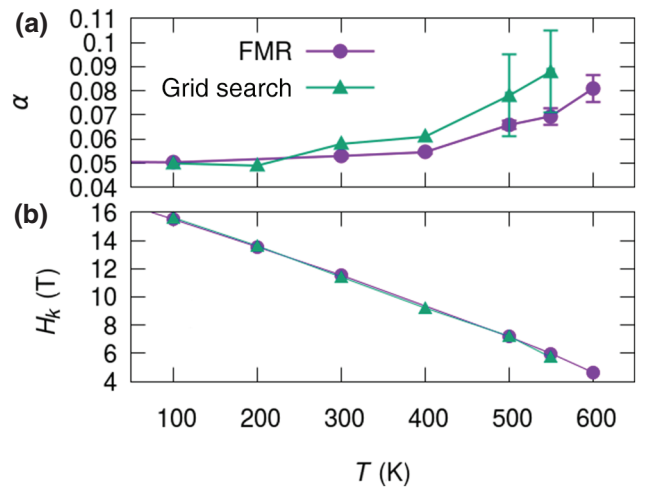


FIG. 3. A comparison of FMR and grid-search fitting: (a) damping; (b) anisotropy.

a system of  $32 \times 32 \times 32$  atoms with periodic boundary conditions. Close to  $T_C$ , the thermal fluctuations become increasingly large for nonperiodic systems and can lead to large errors in the determination of the damping and the anisotropy. For this reason, to reduce the statistical fluctuations, a system of 15 noninteracting grains is modeled. This significantly reduces the fluctuations in the magnetization components and leads to statistically improved results. The in-plane magnetization time series is Fourier transformed and the damping is extracted as presented in Sec. II.

Figure 4 shows the damping as a function of the temperature for bulk and granular systems. For comparison, the temperature is normalized to the Curie temperatures of the systems, which differ due to finite-size effects [21,24]. The granular system will have a reduced Curie temperature due to the cutoff in the exchange interactions at the surface. This is shown as an inset in Fig. 4, where the magnetization as a function of the temperature is computed for the two systems. The Curie temperatures for the two systems, determined from the susceptibility peak, are as follows:  $T_C$  for the grain = 690 K and for the bulk,  $T_C = 720$  K. The input Gilbert damping parameter is 0.05, this value being reproduced at  $T = 0$  K as expected, due to the quenching of magnon excitations.

With increasing temperature, for both bulk and granular systems, the effective damping increases. This can be understood as follows: with enhanced temperature, there is increasing excitation of magnons, which can suffer more complex nonlinear scattering processes.

Moving on to granular systems, the inclusion of the surface will add extra magnon modes into the system, leading

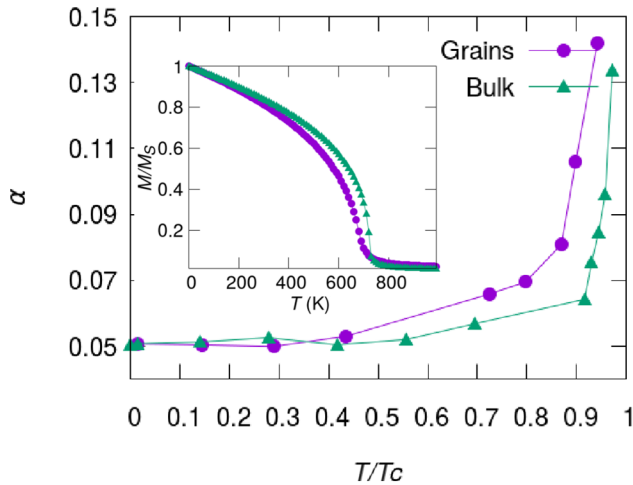


FIG. 4. The damping as a function of the normalized temperature for bulk and granular FePt systems. The granular system shows larger damping overall than the bulk system, due to additional magnon scattering processes at the interface. The inset shows the magnetization curves for granular and bulk FePt. The Curie temperatures for the two systems are as follows: grain,  $T_C = 690$  K; bulk,  $T_C = 720$  K.

to more scattering effects that will increase the effective damping. In order to effect a qualitative illustration of the surface effects, we use the damping calculated from the LLB equation [17]. An analytical solution to the variation of damping with temperature exists in the LLB description, as given by Garanin [17] and Ostler *et al.* [16]. The effective damping as derived within the LLB description is given by

$$\alpha(T) = \frac{\lambda}{m(T)} \left( 1 - \frac{T}{3T_c} \right), \quad (8)$$

where  $\lambda$  is the input coupling to the thermal bath used in the ASD simulations,  $T_C$  is the Curie temperature of the system, and  $m(T) = M(T)/M_s V$  is the normalized magnetization. In principle, Eq. (8) is strictly valid only for an infinite system. However, as a first approximation, finite-size effects can be introduced empirically using diameter-dependent functions  $m(T, D)$  and  $T_c(D)$  calculated using an atomistic model. In the damping calculations considered here, the grain surfaces have two effects. First, the loss of coordination at the surfaces drives a reduction in  $T_c$  and a loss of criticality of the phase transition. This effect can be accounted for by using numerically calculated  $m(T, D)$  and  $T_c(D)$  for a given diameter  $D$ . The second effect is the increased magnon scattering at the surfaces, which is a dynamic effect and is not included in the parametrization of the static properties. Thus it seems reasonable to associate deviations from the parametrized version of Eq. (8) with scattering at the grain surfaces.

Consequently, we compare our numerical results for  $\alpha(T, D)$  with the parametrized version of Eq. (8) - Fig. 5, where  $m(T, D)$  is calculated numerically with the ASD model (shown in Fig. 4, inset) and the Curie temperature [ $T_c(D)$ ] is calculated from the peak of the susceptibility. For the bulk system, the numerical damping calculated from the FMR curves with the atomistic model agrees well

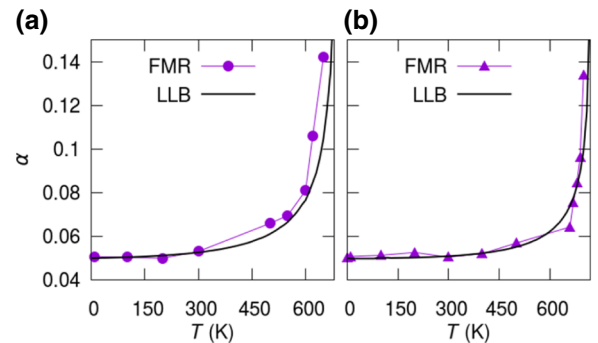


FIG. 5. The damping as a function of the temperature for (a) granular ( $5 \text{ nm} \times 5 \text{ nm} \times 10 \text{ nm}$ ) and (b) bulk systems. The damping calculated via the FMR method is compared against the effective damping from the parametrized LLB formalism given in Eq. (8), where  $m(T, D)$  and  $T_c(D)$  are computed numerically from the atomistic model.

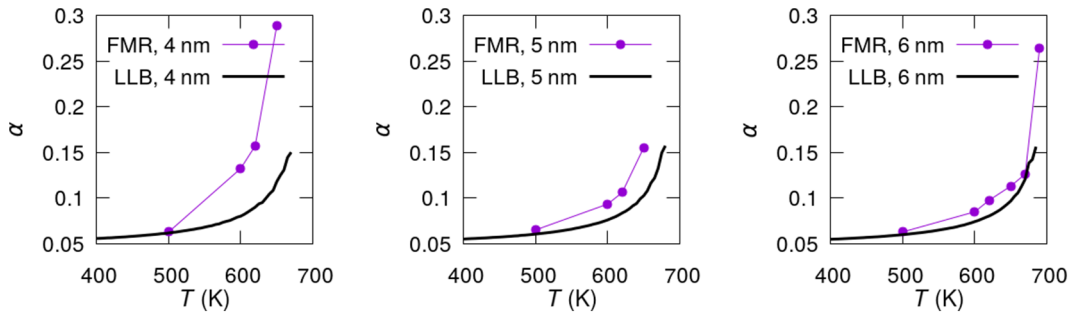


FIG. 6. The temperature dependence of the damping constant for diameters of 4, 5, and 6 nm. The solid lines are calculations using the LLB damping expression. The divergence from the LLB expression for a small particle diameter is indicative of surface effects.

with the damping calculated using the analytical formula given in Eq. (8). This is consistent with the first comparison of atomistic and LLB models [25], which shows that the mean-field treatment of Ref. [17] agrees quantitatively well with atomistic model calculations for the transverse and longitudinal damping. However, the granular system gives a consistently increased damping compared to the analytical formula. Following the earlier reasoning, this enhancement can be attributed to the scattering effects at the grain surface.

To systematically study the effect of the scattering at the surface, we calculate the damping as a function of the system size. For simplicity, we consider cubic grains with a volume varying from 4 nm  $\times$  4 nm  $\times$  4 nm through 5 nm  $\times$  5 nm  $\times$  5 nm to 6 nm  $\times$  6 nm  $\times$  6 nm. Figure 6 shows the damping as a function of the temperature for the different system sizes. With decreasing grain size, the damping is enhanced and systematically diverges further from the LLB analytical damping. The separation of the effects of the finite size on the static and dynamic properties through comparison with the parametrized version of Eq. (8) strongly suggests that this is due to surface scattering of magnons. Clearly, the magnon contributions to the damping give rise to an increase of the damping with increasing temperature, which is inconsistent with the results of Richardson *et al.* [15]. However, the experiments described in Ref. [15] give the temperature dependence of the line width, which likely has contributions from inhomogeneous line broadening arising from dispersion of magnetic properties. In the following, we develop a model accounting for the inhomogeneous line broadening, which gives good qualitative agreement with the experiments.

## V. MODEL INCLUDING INHOMOGENEOUS LINE BROADENING

Realistic granular systems will present a distribution of properties. In the simplest case, the distribution of magnetic properties can arise from a distribution of the size of the grains, which can induce a distribution of  $T_C$ ,  $m$ , and  $H_k$ . Since it is computationally expensive to study a system

of grains numerically within the ASD model, we can, in the first instance, model the effect of the distributions analytically. In the case of a distribution of grains of diameter  $D$ , the power spectrum of the system is expressed by

$$P^{\text{sys}}(f, T) = \int_0^{+\infty} P(f, D, T) F(D) dD. \quad (9)$$

The distribution of size,  $F(D)$ , is considered log-normal. The power spectrum of a grain of diameter  $D$  can be expressed by [16]

$$P(f, B_0, D, T) = C \tilde{m} D^2 \frac{f^2 \gamma B_0^2 \tilde{\alpha}}{(\tilde{\alpha} \tilde{f}_0)^2 + (f - \tilde{f}_0)^2}, \quad (10)$$

where  $\tilde{m} = m(T, D)$ ,  $\tilde{\alpha} = \alpha(T, D)$ ,  $\tilde{f}_0 = f_0(T, D) = \gamma[B_0 + H_k(T, D)]$ , and  $C = \pi h/16$ . This allows us to model both the frequency-swept FMR ( $B_0 = \text{constant}$ ) and the field-swept FMR ( $f = \text{constant}$ ).

We note that a distribution of grain size leads to distributions of further properties, starting, due to finite-size effects, with the Curie temperature. Each of these is introduced into the analytical model as follows. Hovorka *et al.* [21] have shown, via finite-size scaling analysis, that the relation between the size of a grain and its Curie temperature is given by

$$T_C(D) = T_C^\infty (1 - d_0/D)^{1/\nu}, \quad (11)$$

where  $d_0 = 0.71$  and  $\nu = 0.79$  [21] are parametrized for nearest-neighbor exchange systems and  $T_C^\infty = 720\text{K}$ . The variation in  $T_C$  will introduce a variation in the magnetization curves given by

$$m(T, D) = \left(1 - \frac{T}{T_C(D)}\right)^\beta, \beta = 0.33. \quad (12)$$

As a further consequence, the anisotropy will be dependent on the diameter. The uniaxial anisotropy energy  $K$  has a temperature dependence in the form of  $K(T) \sim m(T)^\gamma$ . For

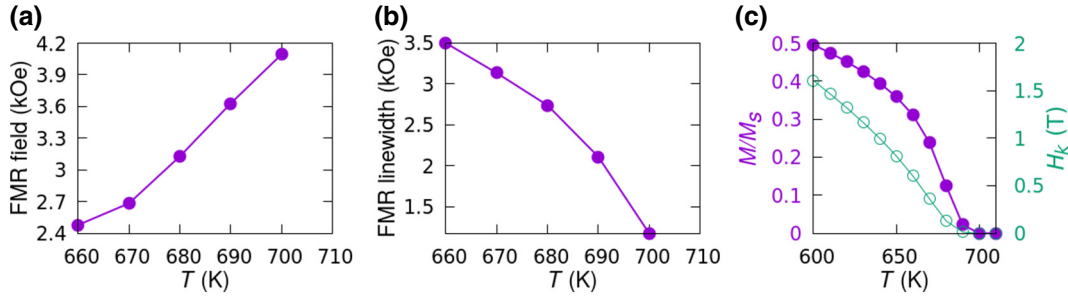


FIG. 7. The field-swept FMR for a log-normal distribution of grains of average diameter  $D = 7$  nm and  $\sigma_D = 0.17$ : input damping  $\lambda = 0.01$ , input  $H_k^0 = 6.6$  T,  $f = 13.7$  GHz. The anisotropy is lower than for bulk FePt to allow resonance at a frequency of 13.7 GHz, corresponding to experiment. The figure shows (a) the variation of the FMR field, (b) the FMR line width ( $\Delta H$ ), and (c) the system magnetization and anisotropy field as a function of the temperature. Close to  $T_C$ , the line width shows a decrease that translates to a decrease in the damping of the system. No magnetostatic or exchange interaction between grains is considered.

FePt, it is found that the exponent is equal to 2.1 by experimental measurements [26,27], in agreement with later *ab initio* calculations [20]. The exponent 2.1 appears for fully ordered  $L1_0$  FePt, due to a dominant two-ion anisotropy term, as shown by Mryasov *et al.* [20], in calculations considering a long-range exchange Hamiltonian parametrized *ab initio*. The granular films presented in Ref. [15] are relatively low anisotropy (around 4 T coercive field at room temperature), which suggests that the two-ion anisotropy is reduced, possibly because of incomplete  $L1_0$  ordering. Hence a scaling exponent of 3 of the uniaxial anisotropy energy [ $K(T) \sim m(T)^3$ ] describes the films presented in Ref. [15] better. The anisotropy field can be expressed as

$$H_K(T, D) = H_K^0 m(T, D)^2. \quad (13)$$

Finally, the size distribution will produce different variations of damping as a function of the grain size, since

$$\alpha(T, D) = \frac{\lambda}{m(T, D)} \left( 1 - \frac{T}{3T_c(D)} \right). \quad (14)$$

In the presence of distributions of properties, the variation of damping with temperature can have a complex behavior, especially close to  $T_c$ , where there is a strong variation of magnetic properties with temperature and size. On reverting to a monodispersed system by setting the distributions to  $\delta$  functions, the damping is given by Eq. (14), resulting in an increase of line width consistent with the temperature Fig. 6.

Richardson *et al.* [15] have shown that, in the case of a granular system of FePt, close to  $T_C$  a decrease in the damping and/or the line width is observed. This effect has been attributed to the competition between two-magnon scattering and spin-flip magnon electron scattering. We show via atomistic-spin-dynamics simulations that surface effects alone cannot be responsible for a decrease in damping, scattering at the surface leading to increased damping at high temperatures.

It is well known that, in the presence of a distribution of properties in the system, the line width broadens. In our case, the distribution of size will lead to a distribution of anisotropy, which increases the line width. Close to the Curie temperature of the system, some grains will become superparamagnetic and will not contribute further to the FMR spectrum; hence it is possible that close to  $T_c$ , the line width can decrease. Figure 7 presents a case in which a decrease in line width appears within 30–40 K of the Curie temperature of the system, a similar temperature interval as spanned by the experimental measurements [15]. Figures 7(a) and 7(b) show the variation of the FMR field and line width as functions of the temperature. The FMR spectra are calculated at a constant frequency of  $f = 13.7$  GHz, consistent with the experimental value used in Ref. [15]. The average magnetization of distributed grains is calculated as

$$M(T) = \frac{\int_0^\infty m(T, D) F(D) D^2 dD}{\int_0^\infty F(D) D^2 dD} \quad (15)$$

and the anisotropy field is calculated as

$$H_K(T) = \int_0^\infty H_K(T, D) F(D) dD. \quad (16)$$

The decrease in line width is associated with the fact that, close to the Curie temperature of the system, the small grains become superparamagnetic and do not contribute to the power spectrum. The loss of the signal from the small grains is especially pronounced due to the enhanced damping of smaller grains.

## VI. CONCLUSIONS AND OUTLOOK

We calculate the temperature dependence of damping and anisotropy for small FePt grain sizes. These parameters are calculated within the ASD framework, via simulation of frequency-swept FMR processes and a

fitting procedure based on the grid-search method. The grid-search method offers a much faster determination of the damping and the anisotropy, parameters crucial for the development of future-generation HAMR drives. The method can be applied both for numerical data as well for experimental relaxation curves obtained via pump-probe experiments. Furthermore, as the magnetic anisotropy energy of FePt is dependent on the chemical disorder and lattice distortion [28], the grid-search method could offer a fast determination of the anisotropy of the system for different FePt systems.

The damping calculations at high temperatures show an increased damping for uncoupled granular systems, as expected due to increased magnon excitation at high temperature. Deviations from the parametrized expression for the temperature dependence of damping from the LLB equation with decreasing grain size suggest that scattering events at grain boundaries enhance the damping mechanism.

This increase in damping, however, is not consistent with the experimental data of Richardson *et al.* [15] which show a decrease in line width at elevated temperatures. We develop a model taking into account the inhomogeneous line broadening arising from the size distribution of the grains, which gives rise to concomitant dispersions of  $T_C$ ,  $m$ , and  $K$ . The model is used to simulate field-swept FMR as used in the experiments. Calculations show that, under the effect of distribution of properties, the line width can exhibit a decrease toward high temperatures, in accordance with the experiments of Ref. [15]. The decrease is predominantly due to a transition to superparamagnetic behavior of small grains with increasing temperature. This suggests inhomogeneous line broadening (likely a significant factor in granular films) as an explanation for the unusual decrease in line width measured by Richardson *et al.* [15]. As large damping is necessary for good performance of HAMR and MRAM devices, with this work we further stress the importance of experimentally controlling the size distributions of the media. Nevertheless, although the results are applied to FePt, the tools developed in this work are general and can be applied to any ferromagnetic granular system.

### ACKNOWLEDGMENTS

We are grateful to Professor M. Wu and Stuart Cavill for helpful discussions. The financial support of the Advanced Storage Research Consortium is gratefully acknowledged. The atomistic simulations were undertaken on the VIKING cluster, which is a high-performance computing facility provided by the University of York. We are grateful for computational support from the University of York High Performance Computing service, VIKING, and the Research Computing team.

- [1] J. C. Slonczewski *et al.*, Current-driven excitation of magnetic multilayers, *J. Magn. Magn. Mater.* **159**, L1 (1996).
- [2] U. Atxitia, T. A. Ostler, R. W. Chantrell, and O. Chubykalo-Fesenko, Optimal electron, phonon, and magnetic characteristics for low energy thermally induced magnetization switching, *Appl. Phys. Lett.* **107**, 192402 (2015).
- [3] H. Y. Yuan, Z. Yuan, K. Xia, and X. R. Wang, Influence of nonlocal damping on the field-driven domain wall motion, *Phys. Rev. B* **94**, 064415 (2016).
- [4] A. Lyberatos and K. Y. Guslienko, Thermal stability of the magnetization following thermomagnetic writing in perpendicular media, *J. Appl. Phys.* **94**, 1119 (2003).
- [5] T. Kobayashi, Y. Nakatani, F. Inukai, K. Enomoto, and Y. Fujiwara, Impact of damping constant on bit error rate in heat-assisted magnetic recording, *J. Magn. Soc. Jpn.* **41**, 52 (2017).
- [6] R. E. Rottmayer, S. Batra, D. Buechel, W. A. Challener, J. Hohlfield, Y. Kubota, L. Li, B. Lu, C. Mihalcea, K. Mountfield, *et al.*, Heat-assisted magnetic recording, *IEEE Trans. Magn.* **42**, 2417 (2006).
- [7] D. Weller, G. Parker, O. Mosendz, E. Champion, B. Stipe, X. Wang, T. Klemmer, G. Ju, and A. Ajan, A HAMR media technology roadmap to an areal density of 4 Tb/in<sup>2</sup>, *IEEE Trans. Magn.* **50**, 1 (2014).
- [8] D. Weller, G. Parker, O. Mosendz, A. Lyberatos, D. Mitin, N. Y. Safonova, and M. Albrecht, Review article: FePt heat assisted magnetic recording media, *J. Vac. Sci. Technol. B* **34**, 060801 (2016).
- [9] M. H. Kryder, E. C. Gage, T. W. McDaniel, W. A. Challener, R. E. Rottmayer, G. Ju, Y-T. Hsia, and M. F. Erden, Heat assisted magnetic recording, *Proc. IEEE* **96**, 1810 (2008).
- [10] J. F. Hu, T. J. Zhou, W. L. Phyoe, Kelvin Cher, and J. Z. Shi, Microstructure control of L1<sub>0</sub> ordered FePt granular film for HAMR application, *IEEE Trans. Magn.* **49**, 3737 (2013).
- [11] J. Becker, O. Mosendz, D. Weller, A. Kirilyuk, J. C. Maan, P. C. M. Christianen, Th Rasing, and A. Kimel, Laser induced spin precession in highly anisotropic granular L1<sub>0</sub> FePt, *Appl. Phys. Lett.* **104**, 152412 (2014).
- [12] K.-D. Lee, H.-S. Song, J.-W. Kim, H. S. Ko, J.-W. Sohn, B.-G. Park, and S.-C. Shin, Gilbert damping and critical real-space trajectory of L1<sub>0</sub>-ordered FePt films investigated by magnetic-field-induction and all-optical methods, *Appl. Phys. Express* **7**, 113004 (2014).
- [13] S. Mizukami, S. Iihama, N. Inami, T. Hiratsuka, G. Kim, H. Naganuma, M. Oogane, and Y. Ando, Fast magnetization precession observed in L1<sub>0</sub>-FePt epitaxial thin film, *Appl. Phys. Lett.* **98**, 052501 (2011).
- [14] N. Mo, J. Hohlfield, M. ul Islam, C. S. Brown, E. Girt, P. Krivosik, W. Tong, A. Rebei, and C. E. Patton, Origins of the damping in perpendicular media: Three component ferromagnetic resonance linewidth in Co-Cr-Pt alloy films, *Appl. Phys. Lett.* **92**, 022506 (2008).
- [15] D. Richardson, S. Katz, J. Wang, Y. K. Takahashi, K. Srinivasan, A. Kalitsov, K. Hono, A. Ajan, and M. Wu, Near- $T_c$  Ferromagnetic Resonance and Damping in FePt-Based Heat-Assisted Magnetic Recording Media, *Phys. Rev. Appl.* **10**, 054046 (2018).
- [16] T. A. Ostler, M. O. A. Ellis, D. Hinzke, and U. Nowak, Temperature-dependent ferromagnetic resonance via the



- Landau-Lifshitz-Bloch equation: Application to FePt, *Phys. Rev. B* **90**, 094402 (2014).
- [17] D. A. Garanin, Fokker-Planck and Landau-Lifshitz-Bloch equations for classical ferromagnets, *Phys. Rev. B* **55**, 3050 (1997).
- [18] R. F. L. Evans, W. J. Fan, P. Chureemart, T. A. Ostler, M. O. A. Ellis, and R. W. Chantrell, Atomistic spin model simulations of magnetic nanomaterials, *J. Phys. Condens. Matter* **26**, 103202 (2014).
- [19] M. O. A. Ellis, R. F. L. Evans, T. A. Ostler, J. Barker, U. Atxitia, O. Chubykalo-Fesenko, and R. W. Chantrell, The Landau-Lifshitz equation in atomistic models, *Low Temp. Phys.* **41**, 705 (2015).
- [20] O. N. Mryasov, U. Nowak, K. Y. Guslienko, and R. W. Chantrell, Temperature-dependent magnetic properties of FePt: Effective spin Hamiltonian model, *EPL* **69**, 805 (2005).
- [21] O. Hovorka, S. Devos, Q. Coopman, W. J. Fan, C. J. Aas, R. F. L. Evans, Xi Chen, G. Ju, and R. W. Chantrell, The Curie temperature distribution of FePt granular magnetic recording media, *Appl. Phys. Lett.* **101**, 052406 (2012).
- [22] M. O. A. Ellis, T. A. Ostler, and R. W. Chantrell, Classical spin model of the relaxation dynamics of rare-earth doped permalloy, *Phys. Rev. B* **86**, 174418 (2012).
- [23] Sutee Sampan-a-pai, Jessada Chureemart, Roy W. Chantrell, Roman Chepulskeyy, Shuxia Wang, Dmytro Apalkov, Richard F. L. Evans, and Phanwadee Chureemart, Temperature and Thickness Dependence of Statistical Fluctuations of the Gilbert Damping in Co-Fe-B/MgO Bilayers, *Phys. Rev. Appl.* **11**, 044001 (2019).
- [24] A. Lyberatos, D. Weller, G. J. Parker, and B. C. Stipe, Size dependence of the Curie temperature of L1<sub>0</sub> - FePt nanoparticles, *J. Appl. Phys.* **112**, 113915 (2012).
- [25] O. Chubykalo-Fesenko, U. Nowak, R. W. Chantrell, and D. Garanin, Dynamic approach for micromagnetics close to the Curie temperature, *Phys. Rev. B* **74**, 094436 (2006).
- [26] J.-U. Thiele, K. R. Coffey, M. F. Toney, J. A. Hedstrom, and A. J. Kellock, Temperature dependent magnetic properties of highly chemically ordered Fe<sub>55-x</sub>Ni<sub>x</sub>Pt<sub>45</sub>L1<sub>0</sub> films, *J. Appl. Phys.* **91**, 6595 (2002).
- [27] S. Okamoto, N. Kikuchi, O. Kitakami, T. Miyazaki, Y. Shimada, and K. Fukamichi, Chemical-order-dependent magnetic anisotropy and exchange stiffness constant of FePt (001) epitaxial films, *Phys. Rev. B* **66**, 024413 (2002).
- [28] C. J. Aas, L. Szunyogh, J. S. Chen, and R. W. Chantrell, Magnetic anisotropy of FePt: Effect of lattice distortion and chemical disorder, *Appl. Phys. Lett.* **99**, 132501 (2011).